ARIMA-Based Time Series Model of Stochastic Wind Power Generation

Chen, Peiyuan; Pedersen, Troels; Bak-Jensen, Birgitte; Chen, Zhe

Published in:
IEEE Transactions on Power Systems

DOI (link to publication from Publisher):
10.1109/TPWRS.2009.2033277

Publication date:
2010

Document Version
Publisher's PDF, also known as Version of record

ARIMA-Based Time Series Model of Stochastic Wind Power Generation

Peiyuan Chen, *Student Member, IEEE*, Troels Pedersen, *Student Member, IEEE*, Birgitte Bak-Jensen, *Member, IEEE*, Zhe Chen, *Senior Member, IEEE*

***Abstract*-- This paper proposes a stochastic wind power model based on an autoregressive integrated moving average (ARIMA) process. The model takes into account the nonstationarity and physical limits of stochastic wind power generation. The model is constructed based on wind power measurement of one year from the Nysted offshore wind farm in Denmark. The proposed limited-ARIMA (LARIMA) model introduces a limiter and characterizes the stochastic wind power generation by mean level, temporal correlation and driving noise. The model is validated against the measurement in terms of temporal correlation and probability distribution. The LARIMA model outperforms a first-order transition matrix based discrete Markov model in terms of temporal correlation, probability distribution and model parameter number. The proposed LARIMA model is further extended to include the monthly variation of the stochastic wind power generation.**

***Index Terms*--ARIMA processes, Markov processes, stochastic processes, time series, wind power generation.**

I. Introduction

THE high integration of wind power into electrical systems calls for new methods and simulation tools that can assist electric utilities in analyzing the impact of stochastic wind power generation on power system operation and planning [1]. Such analyses usually require a probabilistic approach, which commonly relies on sequential Monte Carlo simulations [2]. The sequential Monte Carlo simulations consider both the probability distribution and chronological characteristics of wind power generation, load profiles, and transition states of all the system components [2]. Furthermore, the sequential Monte Carlo simulations usually require a large number of simulation runs to obtain statistically reliable results, for instance to capture rare events such as extreme wind situations. Thus, stochastic wind power models that are able to capture both the probability distribution and temporal correlation of the wind power generation are needed.

As depicted in Fig. 1, existing approaches for the stochastic modeling of the wind power generation fall into two categories: the wind speed approach [3]-[8] and the wind power approach [9]. Both approaches are based on wind speed measurements. The former approach requires a wind speed model. The available wind speed models include the autoregressive moving average (ARMA) model [3], [4], the discrete Markov model [5]-[7], and the wavelet-based model [8]. In contrast, the latter approach requires a wind power model. The available wind power model in [9] uses a transition matrix based discrete Markov model.

The two approaches can be applied to planning of future wind farms in the power system. However, both approaches entail wind speed measurements and an accurate wind farm model, which is usually unavailable. The accurate wind farm model is not needed in the case where wind power measurements are available. In fact, electric utilities measure and record wind power flowing into their networks. Thus, they have direct access to these wind power data. In this case, as shown in Fig. 1, wind power measurements can be directly used to build a wind power model, which may be used for system planning involving already operating wind farms. In addition, the need for wind speed measurements is alleviated.

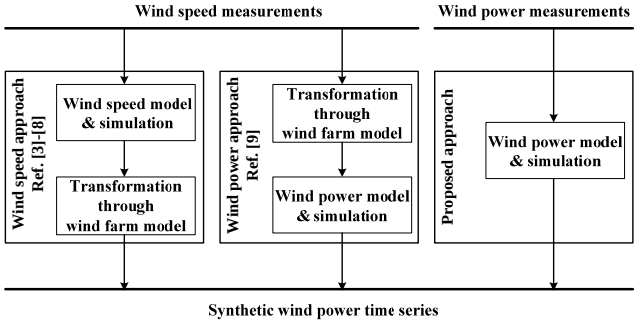

Fig. 1. Alternative approaches for modeling wind power time series.

In the case that only wind speed measurements are available, either approaches may be applied. One disadvantage of the wind power approach is that wind power generation has both lower and upper limits and does not follow a standard probability distribution. These make it more challenging to apply standard statistical models. On the other hand, one drawback of the wind speed approach is that an error, e.g. of 3%, in wind speed modeling may cause an error of around 9% in wind power. This is because wind power varies with cube of wind speed when the speed is between cut in and rated value.

In brief, the challenges of building the stochastic wind power model are that the wind power generation is a

This work was supported by the Danish Agency for Science Technology and Innovation, under the project of 2104-05-0043.

P. Chen, B. Bak-Jensen and Z. Chen are all with the Department of Energy Technology, Pontoppidanstraede 101, Aalborg University, Aalborg, 9220 Denmark (e-mail: pch@iet.aau.dk, zch@iet.aau.dk, bbj@iet.aau.dk).

T. Pedersen is with the Department of Electronic Systems, Section Navigation and Communications, Aalborg University, Fredrik Bajers Vej 7, Aalborg, 9220 Denmark (e-mail: troels@es.aau.dk).

nonstationary and non-Gaussian random process, where a direct application of ARMA models is not feasible. As proposed in [9], the discrete Markov model using transition matrix may be applied to modeling the wind power generation. This model is constructed based on a quantized wind power time series. The transition matrix defines probabilities of moving from one state to any other states. However, the model presents several practical problems. Firstly, the model does not consider the nonstationary characteristic of the wind power generation. Secondly, the model requires a large number of parameters and thus calls for a large amount of training data. Finally, the model gives a poor fit with respect to probability distribution. This lack-of-fit is due to the error induced when quantizing the wind power time series.

This paper proposes a parsimonious stochastic wind power model based on an autoregressive integrated moving average (ARIMA) model. The proposed model takes into account the nonstationary characteristic of the wind power generation with only few model parameters. In addition, the proposed model does not rely on quantization and thus does not suffer from quantization errors.

The rest of the paper is organized as follows. Section II introduces necessary notations and concepts. Section III performs a statistical analysis on a one-year wind power time series measured from the Nysted offshore wind farm in Denmark. A standard ARIMA model for the measurement data is then identified in section IV. Section V improves the identified ARIMA model by introducing a limiter to the feedback loop of the model. The proposed model, referred to as the limited-ARIMA (LARIMA) model, is further extended to include the monthly variations of the wind power generation. Concluding remarks and future works are stated in section VI.

II. Methodology

This section presents the necessary notations and concepts of stationary and nonstationary random processes. Then, the ARIMA model for the nonstationary random process is introduced and the Box-Jenkins' procedures of model identification for a nonstationary time series is outlined. Interested readers are referred to [11], [12] for detailed information.

A. Wide-Sense Stationary and Nonstationary Random Process

Let $y(1), \ldots, y(\mathrm{N})$ denote an observed time series, which is modeled by a random process $Y(t)$. The temporal correlation of the random process can be described by the autocorrelation coefficient (ACC) [13] and partial autocorrelation coefficient (PACC). The ACC expresses the linear correlation of data among adjacent observations of a random process. The theoretical ACC of a random process is usually not known, but can be estimated from the observed time series by the sample ACC as [12]

$$\hat{\rho}_Y(k) = \frac{\frac{1}{\mathrm{N}-k}\sum_{i=1}^{\mathrm{N}-k}\left[y(i)y(i+k)\right] - \hat{m}_Y^2}{\hat{\sigma}_Y^2}, \text{ for } k = 0,1,\ldots \mathrm{N}-1 \quad (1)$$

where $\hat{m}_Y$ and $\hat{\sigma}_Y^2$ are the sample mean and variance of the observed time series, respectively.

The PACC of $Y(t)$ describes the correlation between $Y(t)$ and $Y(t+k)$ when the mutual linear dependency of $Y(t+1)$, $Y(t+2)$, …, $Y(t+k-1)$ is removed. In other words, it is the correlation between $Y(t)$ and $Y(t+k)$ conditioned on $Y(t+1)$, $Y(t+2)$, …, $Y(t+k-1)$. Given the sample ACC, the sample PACC $\hat{\gamma}_Y(k)$ can be calculated iteratively through [12]

$$\hat{\gamma}_Y(k+1) = \frac{\hat{\rho}_Y(k+1) - \sum_{j=1}^{k}\hat{\gamma}_Y(k,j)\,\hat{\rho}_Y(k+1-j)}{1 - \sum_{j=1}^{k}\hat{\gamma}_Y(k,j)\,\hat{\rho}_Y(j)}, \quad (2)$$

where $\hat{\gamma}_Y(0) = 1$, and

$$\hat{\gamma}_Y(k,j) = \hat{\gamma}_Y(k-1,j) - \hat{\gamma}_Y(k)\,\hat{\gamma}_Y(k-1,k-j). \quad (3)$$

The standard error of the sample PACC is approximated by [12]

$$S_{\mathrm{PACC}} = \sqrt{1/\mathrm{N}}. \quad (4)$$

Hence, $\pm 2S_{\mathrm{PACC}}$ can be used as critical limits on the sample PACC to test the hypothesis of a white noise process.

With respect to the WSS random process, a nonstationary random process $Y(t)$ distinguishes itself in a number of ways. It may have a time-varying mean $m_Y(t)$ and variance $\sigma_Y^2(t)$. Some transformations, such as differencing and variance-stabilizing [12], are introduced to transform the nonstationary random process to an approximately stationary one.

For a process with the time-varying mean, a stochastic trend model can be applied [12]. The stochastic trend model is constructed by differencing the random process for d times, i.e.

$$Z(t) = (1-B)^d\, Y(t), \quad (5)$$

where B is the backshift operator such that $B^j Y(t) = Y(t-j)$.

For a process with the time-varying variance, the Box-Cox's power transformation is applied to stabilize the variance by [12]

$$\mathrm{T}\left(Y(t)\right) = \frac{Y^{\nu}(t)-1}{\nu\,\mathrm{G}^{\nu-1}(Y)}, \quad (6)$$

where G(Y) is the geometric mean of $Y(1)$, …, $Y(\mathrm{N})$:

$$\mathrm{G}(Y)=\left(\prod_{i=1}^{\mathrm{N}} Y(i)\right)^{1/\mathrm{N}}, \tag{7}$$

and v is a parameter determining the transformation. The criterion for selecting v for variance stabilizing transformation is to minimize the residual sum of squares [12]

$$SS(v)=\sum_{t=1}^{\mathrm{N}}\left(\mathrm{T}\left(y(t)\right)-\hat{m}_Y\right)^2. \tag{8}$$

Some common transformations are listed in Table I together with the corresponding v. The values of $\ln(SS(v))$ are calculated from the wind power measurements presented in the following section and will be further discussed in Section IV. The power transformation is usually applied before the differencing operation.

TABLE I
BOX-COX POWER TRANSFORMATION [12] AND LOGARITHM OF THE RESIDUAL SUM OF SQUARES OF THE POWER-TRANSFORMED WIND POWER TIME SERIES

v	Transformation	$\ln(SS(v))$
-1	$1/Y(t)$	38.5
-0.5	$1/\sqrt{Y(t)}$	26.1
0	$\ln Y(t)$	16.6
0.5	$\sqrt{Y(t)}$	15.5
1	$Y(t)$	17.1

B. The ARIMA-family model

An ARIMA(p, d, q) model of the nonstationary random process $Y(t)$ is expressed as [12]

$$\left(1-\sum_{i=1}^{p}\varphi_i B^i\right)(1-B)^d\, Y(t)=\theta_0+\left(1-\sum_{i=1}^{q}\theta_i B^i\right)a(t) \tag{9}$$

where $\{\varphi_i\}$ are the AR coefficients; $\{\theta_i\}$ are the moving average (MA) coefficients; $a(t)$ is a white Gaussian process with zero mean and variance σ_a^2; the parameter θ_0 is referred to as the deterministic trend term when $d>0$. The deterministic trend term θ_0 can be omitted unless the sample mean $\hat{m}_Z$ of the transformed time series $Z(t)$ as in (5) is significantly larger than its standard error $S\left(\hat{m}_Z\right)$ [12]. The standard error can be approximated by

$$S\left(\hat{m}_Z\right)=\sqrt{\sigma_Z^2\left(1+2\hat{\rho}_Z(1)+2\hat{\rho}_Z(2)+\cdots+2\hat{\rho}_Z(k)\right)/\mathrm{N}}, \tag{10}$$

where σ_Z^2 is the sample variance of $Z(t)$ and $\hat{\rho}_Z(1),\ldots,\hat{\rho}_Z(k)$ are the first k significant sample ACCs of $Z(t)$.

In the case of $d=0$, the ARIMA(p, d, q) model is reduced to an ARMA(p, q) model [12]. For an ARMA model, θ_0 is related to the sample mean $\hat{m}_Y$ of the process as

$$\theta_0=\hat{m}_Y\left(1-\varphi_1-\cdots-\varphi_p\right). \tag{11}$$

The ARMA(p, q) model is reduced to an AR(p) model when $q=0$, and an MA(q) model when $p=0$. The coefficients of the ARMA model can be estimated by the Yule-Walker estimator, the least square estimator, the maximum likelihood estimator, etc [12].

The Box-Jenkins's procedures of model identification for a nonstationary time series [12] are summarized in four steps:

- Choose proper transformations of the observed time series. The most common transformations are variance-stabilizing transformation and differencing operation.
- Calculate the sample ACC and PACC of the observed time series to decide the necessity and degree of differencing.
- Calculate the sample ACC and PACC of the properly transformed time series to identify the orders of p and q of the ARIMA model.
- Test the deterministic trend term θ_0 if $d>0$ to decide the necessity of including θ_0 in the model.

The Box-Jenkins' procedures of model identification will be followed in section IV, after the analysis of the measured wind power time series in section III.

III. STATISTICAL ANALYSIS OF WIND POWER TIME SERIES

A statistical analysis is performed on a wind power time series measured from the Nysted offshore wind farm connected to the Lolland-Falster distribution system in Denmark. The wind farm's capacity is 165.6 MW. It consists of 72 fixed-speed wind turbines, each with capacity of 2.3 MW. The data are hourly measurements from Jan. 1 to Dec. 31, 2005.

The time-domain plots of the wind power time series for the whole year and first ten days in January are shown in Fig. 2. The wind power generation is on average higher in certain months (Nov. to Apr.) than in other months (May to Oct.). A strong temporal correlation is observed, e.g. a continuously high power generation between 48$^{\text{th}}$ h and 96$^{\text{th}}$ h. However, a dramatic change in power generation from almost maximum to zero is also observed between 168$^{\text{th}}$ h and 192$^{\text{nd}}$ h.

The empirical probability density function of the measured time series is shown in Fig. 3. The probability mass concentrates around zero of the distribution and shows a small rise around the rated power. This effect is expected from the actual operation of the wind farm due to power limitations at the cut-in and rated wind speed. As a result, the distribution is not a standard exponential or any other standard probability distribution.

The sample ACC and PACC of the measured time series are shown in Fig. 4. The sample ACC decays slowly. The sample PACC is significant for time lags up to 3. According to [12], this indicates that the time series may be nonstationary. The implication of the sample ACC and PACC on the model identification is to be discussed in section IV.

The periodogram [14] of the time series is shown in Fig. 5. No particularly dominant frequency components are observed. The frequency component corresponding to 24 h is present, but very weak. Thus, it will not be considered in the sequel.

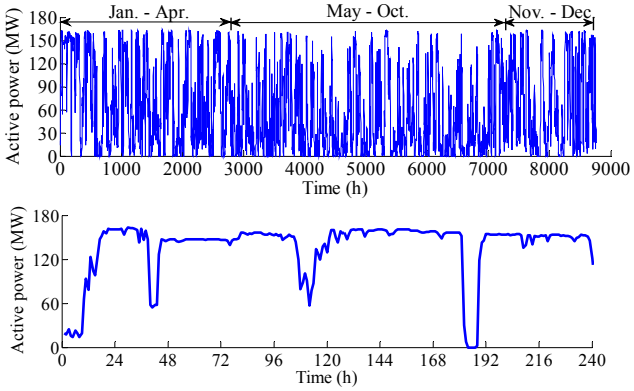

Fig. 2. Wind power time series from measurements: one-year time series (top), and first ten days in January (bottom)

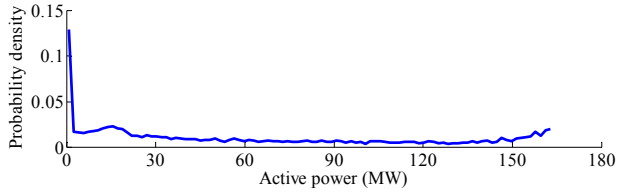

Fig. 3. Empirical probability density of the measured wind power time series.

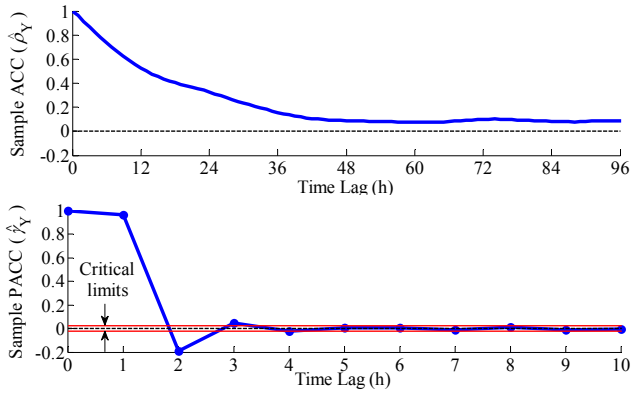

Fig. 4. Sample ACC (upper) and PACC (lower) of the measured wind power time series.

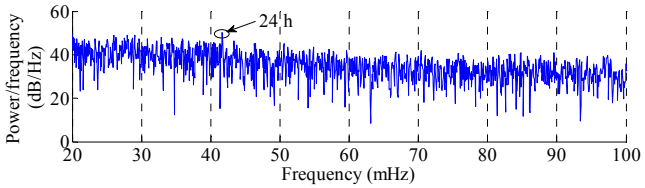

Fig. 5. Periodogram of the measured wind power time series.

IV. ARIMA Model of Wind Power Time Series

In this section, ARIMA models are identified for the wind power data described in section III based on the Box-Jenkins' procedures. Then, the model diagnostic and selection on the identified models are carried out. Finally, the deficiency of the selected models is discussed.

A. Model Identification

The computed natural logarithm of the residual sum of squares of the wind power data according to (8) is summarized in Table I for different values of the transformation parameter v. The results indicate that a square-root transformation ($v = 0.5$) has the smallest residual sum of squares, and should therefore be applied to the data.

As shown in Fig. 4, the sample ACC of the measured time series decays slowly, while the sample PACC damps off after lag 3. This indicates that the differencing is needed [12]. With one degree of differencing on the square root of the measured time series, the resulting transformed time series is shown in Fig. 6. The time series now appears to be approximately stationary. The sample ACC and PACC of the transformed time series are shown in Fig. 7. The sample ACC cuts off after time lag 1 and the sample PACC damps off after time lag 2. This matches with an MA(1) model with a negative θ_1 [12]. Fitting the MA(1) model directly on the transformed wind power time series gives $\theta_1 = -0.224$ and $\sigma_a^2 = 1.172$. The theoretical ACC of an MA(1) model is calculated by [11]

$$\rho(k) = \begin{cases} 1, & k=0 \\ -\theta_1 \big/ \left(1+\theta_1^2\right), & k=1 \\ 0, & k \geq 2 \end{cases}. \tag{12}$$

The corresponding values of PACC can be obtained using (2). The theoretical ACC and PACC of the MA(1) model with $\theta_1 = -0.224$ are shown as the dashed lines in Fig. 7. The sample ACC and PACC of the transformed time series matches with the corresponding theoretical values of the MA(1) model.

The sample mean of the transformed time series (after square-root and differencing) is $\hat{m}_Z = -2.0547\times10^{-5}$. According to (10), the standard error is $S\left(\hat{m}_Z\right) = 0.0203$, which is much larger than the sample mean. Thus, the deterministic trend term θ_0 is insignificant and can be omitted from the model.

Consequently, the following ARIMA(0,1,1) model is entertained for the wind power time series. It is a first-order integrated MA model.

$$\begin{cases} (1-B)I_0(t) = (1-\theta_1 B)a(t) \\ Y(t) = I_0^2(t) \end{cases}, \qquad \text{for } t = 1, \ldots, N, \tag{13}$$

The block diagram of the model is shown in Fig. 8, where the back shifter B is the same as a unit delay. The estimated parameters, θ_1 and σ_a^2, are listed in Table II.

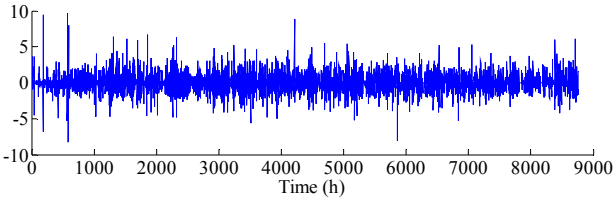

Fig. 6. Square root followed by one-order differencing of measured time series.

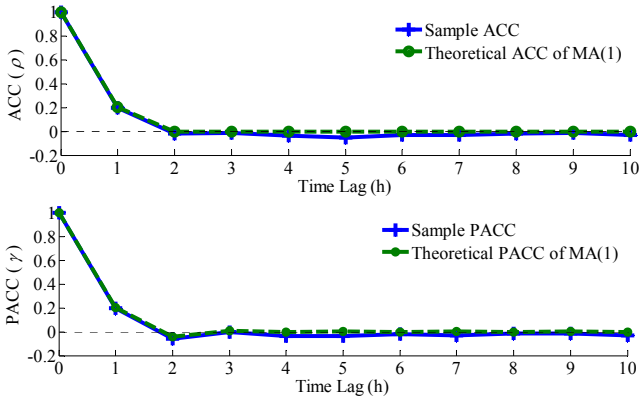

Fig. 7. ACC (upper) and PACC (lower): transformed wind power time series (solid) and MA(1) model with θ_1 = -0.2241 (dashed).

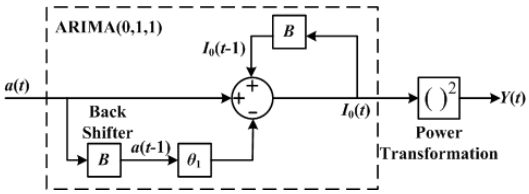

Fig. 8. Block diagram of ARIMA(0,1,1) model of wind power time series.

TABLE II
PARAMETER ESTIMATES FOR THE ARIMA(0,1,1) AND ARMA(1,1) MODELS

Model	φ_1	θ_0	θ_1	σ_a^2
ARIMA(0,1,1)	—	—	−0.224	1.172
ARMA(1,1)	0.971	0.197	−0.241	1.148

B. Model Diagnostic and Selection

The model diagnostic is required to assess the adequacy of the model by checking whether or not the model assumption is valid. The fundamental assumption is that the residual $a(t)$ is a white noise [11], i.e. an uncorrelated random process with zero mean and constant variance. The residual $a(t)$ is obtained by

$$a(t) = (1-B)\sqrt{y(t)} + \theta_1 a(t-1) \tag{14}$$

The Box-Cox power transformation of the residual indicates that the residual sum of square is minimized when no transformation is applied. This indicates a constant variance of the residual [12]. The sample ACC and PACC of the residual are shown in Fig. 9. The values at lag 0 are equal to 1 and not shown. The sample ACC and PACC do not exhibit any obvious pattern and are generally within the critical limits. This indicates an uncorrelated random process. Therefore, the white noise assumption of the residual is found to be valid.

Although the ARIMA(0,1,1) model according to the preceding analysis is assessed to be an adequate model for the wind power time series, there may be several other adequate models as well. For example, higher-order ARIMA(p,1,q) models with $p > 0$ and $q > 1$. In addition, as shown in Fig. 8, the coefficient of the feedback of $I_0(t)$ is 1, corresponding to one degree of differencing. If the coefficient is varied within (0, 1), the model becomes an ARMA(1,1) model, which also shows a good modeling in ACC and PACC. The ARMA(1,1) model is expressed as

$$\begin{cases} (1-\varphi_1 B) I_0(t) = \theta_0 + (1-\theta_1 B) a(t) \\ Y(t) = I_0^2(t) \end{cases}, \qquad \text{for } t = 1, \ldots, \mathrm{N}, \tag{15}$$

where the estimated parameters, φ_1, θ_0, θ_1 and σ_a^2, are listed in Table II. Consequently, the problem in this case becomes selecting one among models of varying complexity.

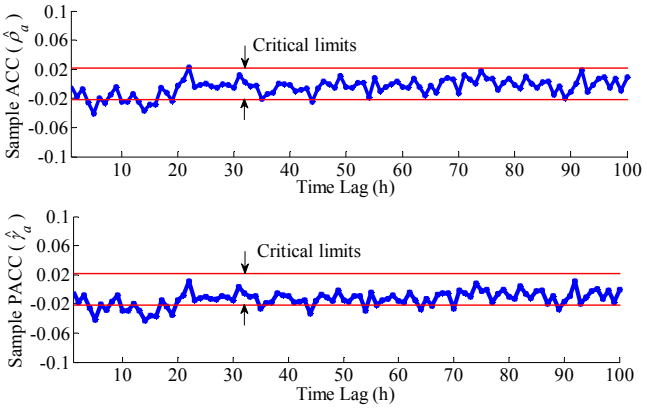

Fig. 9. Sample ACC and PACC of the residual of the ARIMA(0,1,1) model.

Model selection criteria based on residuals are applied to choose the best model among the adequate ones. The common selection criteria are Akaike's information criterion (AIC) and Bayesian information criterion (BIC). The AIC of the ARIMA model is defined as [12]

$$\mathrm{AIC}(M) = \mathrm{N} \ln \sigma_a^2 + 2M, \tag{16}$$

where M is the number of parameters in the model. The optimal order of the model is chosen by the value of M, so that AIC(M) is minimum. The parameters and AIC values of five adequate ARIMA models are summarized in Table III.

The ARMA(1,1) model yields the smallest AIC value whereas the ARIMA(0,1,1) model gives the second smallest AIC value. It turns out that the AIC criterion favors the ARMA(1,1) model with 4 parameters instead of the ARIMA(0,1,1) model with 2 parameters. The BIC criterion leads to a similar conclusion. In fact, the ARMA(1,1) model resembles with the ARIMA(0,1,1) model as φ_1 is close to unity. This also implies that the time series may be

nonstationary. In addition, the ARIMA(0,1,1) model requires less parameters. Hence, both the ARMA(1,1) and ARIMA(0,1,1) model are considered to be candidate models.

TABLE III
AIC CRITERIA OF DIFFERENT ARIMA MODELS

Model	Parameters	M	σ_a^2	AIC
ARMA(1,1)	$\varphi_1, \theta_0, \theta_1, \sigma_a^2$	4	1.1483	1219
ARIMA(0,1,1)	θ_1, σ_a^2	2	1.1717	1392
ARIMA(0,1,2)	$\theta_1, \theta_2, \sigma_a^2$	3	1.1721	1397
ARIMA(1,1,1)	$\varphi_1, \theta_1, \sigma_a^2$	3	1.1721	1397
ARIMA(1,1,0)	φ_1, σ_a^2	2	1.1759	1423

C. Model Deficiency

Due to the physical limitations of the wind farm, the wind power generation is bounded within [0, 165.6] MW. However, neither the ARMA nor the ARIMA model considers these limitations. The mean and variance of the ARMA(1,1) model are calculated by [11]

$$\begin{cases} m_{I_0} = \theta_0 / (1-\varphi_1) \approx 6.7 \\ \sigma_{I_0}^2 = \sigma_a^2 \left(1+\theta_1^2 - 2\varphi_1\theta_1\right) / \left(1-\varphi_1^2\right) \approx 30.0 \end{cases}. \tag{17}$$

However, the sample mean and variance of the square-root transformed wind power data are 6.7 and 16.5, respectively. The ARMA(1,1) model fits the measurement in terms of the mean but not the variance. The variance of the ARIMA(0,1,1) model does not converge and increases as time proceeds due to its nonstationarity property. The discrepancy in the variance indicates that the standard ARMA or ARIMA model cannot be directly applied to a bounded random process. The following proposes a new model for the bounded random process.

V. PROPOSED MODEL OF WIND POWER TIME SERIES

This section first proposes four modified ARMA and ARIMA models, referred to as the ARMA model with limiter, ARIMA model with limiter, LARMA model and LARIMA model, respectively, for the bounded wind power time series. Then, the model that has the best fit in probability distribution is selected. Moreover, the selected model is compared with a transition matrix based discrete Markov model in terms of probability distribution and temporal correlation. Finally, the selected model is extended to include the monthly variation of the wind power generation.

A. Modified ARMA and ARIMA Models

Since the wind power output is bounded, a limiting operation is introduced as

$$I(t) = \begin{cases} \mathrm{I}_{\max}, & I_0(t) > \mathrm{I}_{\max} \\ I_0(t), & \mathrm{I}_{\min} \le I_0(t) \le \mathrm{I}_{\max} \\ \mathrm{I}_{\min}, & I_0(t) < \mathrm{I}_{\min} \end{cases}. \tag{18}$$

where $\mathrm{I}_{\max}$ and $\mathrm{I}_{\min}$ denote the upper and lower bounds of the square root of the wind power output, respectively. For the considered wind farm, the wind power output is bounded within [0, 165.6] MW, yielding $\mathrm{I}_{\max} = \sqrt{165.6} = 12.87$ and $\mathrm{I}_{\min} = 0$. Consequently, the wind power time series can be simulated by

$$Y(t) = I^2(t), \qquad \text{for } t = 1, ..., \mathrm{N}. \tag{19}$$

The limiter may be included outside or inside the feedback loop of $I_0(t)$ shown in Fig. 8. The model with the limiter outside the feedback loop is shown in Fig. 10 (a). The model is referred to as the ARMA model with limiter when $0 < \varphi_1 < 1$, and the ARIMA model with limiter when $\varphi_1 = 1$. The model with the limiter inside the feedback loop is shown in Fig. 10 (b). The model is referred to as the LARMA model when $0 < \varphi_1 < 1$, and the LARIMA model when $\varphi_1 = 1$, with 'L' indicating the introduction of the limiter.

Due to the nonstationarity of an ARIMA model, its mean and variance diverge as time proceeds [11]. With the inclusion of the limiter, however, the mean and variance of the LARIMA model is bounded. Consider two extreme cases when σ_a^2 approaches zero and infinity while $\theta_0 = 0$. It is not difficult to derive that the mean and variance of $I(t)$ in the LARIMA model is bounded as:

$$\begin{cases} 0 \le m_I \le \mathrm{I}_{\max}/2 \\ 0 \le \sigma_I^2 \le \mathrm{I}_{\max}^2/4 \end{cases}. \tag{20}$$

Therefore, a modification is required to control the mean of the model. In other words, a deterministic trend term must be included. The value of θ_0 is adjusted until the sample mean of $Y(t)$ coincides with that of the measured time series $y(t)$. The variance is automatically adjusted as it is the autocorrelation at time lag zero minus the square of the mean. According to the simulation, $\theta_0 = 0.011$ for the LARIMA model.

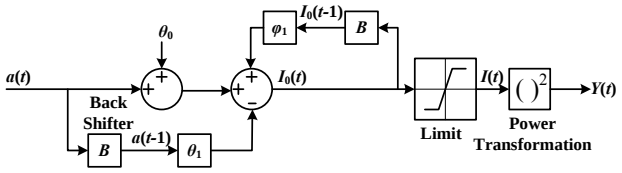

(a) ARMA(1,1) with limiter ($0 < \varphi_1 < 1$), ARIMA(0,1,1) with limiter ($\varphi_1 = 1$).

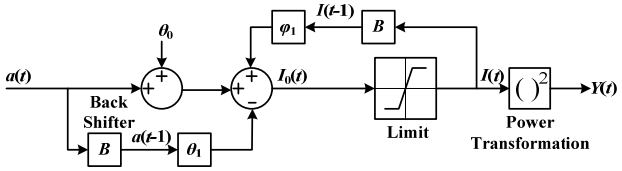

(b) LARMA(1,1) ($0 < \varphi_1 < 1$), LARIMA(0,1,1) ($\varphi_1 = 1$).

Fig. 10. Block diagrams of four ARIMA-type wind power time series models.

B. Model Selection

The selection among the ARMA model with limiter, the

ARIMA model with limiter, the LARMA model, and the LARIMA model depends on which one providing the best fit in probability distribution.

In order to compare the probability distribution of the four models, the quantile values of the time series simulated from the models are plotted against those from the original measurement data as shown in Fig. 11 (a)-(d). Each plot is computed from 100 independently generated time series of 8760 samples The quantile-quantile plot is a standard means of comparing probability distributions. Different quantiles correspond to values of a cumulative distribution function at different probabilities. If the simulated time series and the measured one are from the same probability distribution, then the quantile-quantile plot follows a straight line with a unit slope (the solid line in the figure).

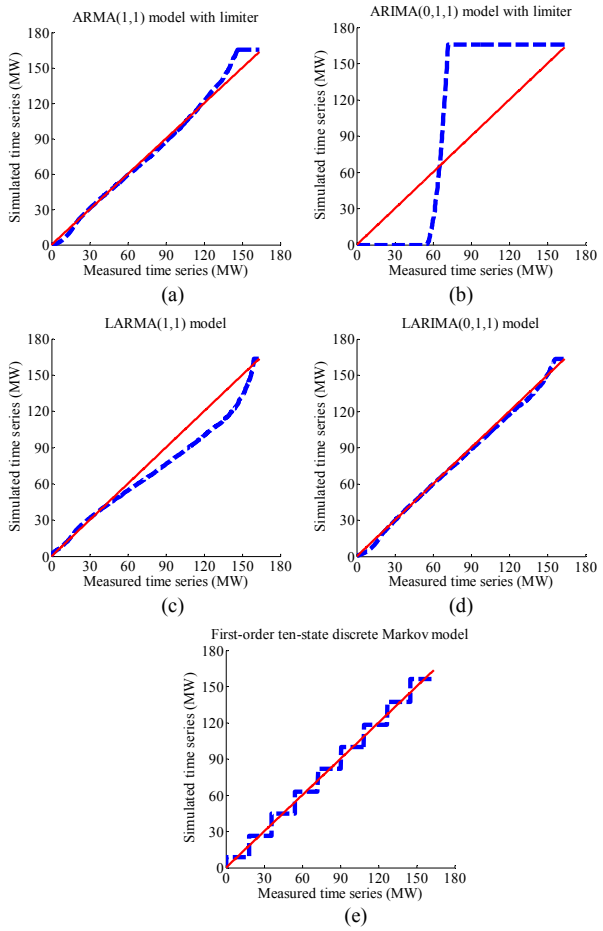

Fig. 11. Quantile-quantile plots of simulated time series from six models against the measured time series (dashed line), and straight lines with unit slope (solid line).

It is observed from Fig. 11 (a) that the ARMA(1,1) model with limiter fits well for quantiles less than 120 MW, but fits poorly in the higher power region. The ARIMA(0,1,1) model with limiter shown in Fig. 11 (b) shows a poor fit in all quantiles. This observation indicates that the simulated values from the ARIMA(0,1,1) model with limiter hit the upper and lower limit most of the time. This effect is caused by the nonstationarity characteristic of the ARIMA model. The LARMA(1,1) model in Fig. 11 (c) also deviates evidently from the straight line and gives a poor fit in probability distribution. The LARIMA(0,1,1) model in Fig. 11 (d) gives the best fit among the four models. Due to the importance of the accuracy in probability distribution of wind power generation, the LARIMA(0,1,1) is favored among the four modified ARMA and ARIMA models. Thus, the LARIMA(0,1,1) model is finally selected as the best model for modeling the wind power time series. Fig. 11 (e) is to be discussed in the following subsection.

C. LARIMA model vs. Discrete Markov Model

The LARIMA(0,1,1) model proposed in this paper is compared with the first-order transition matrix based discrete Markov model proposed in [9]. The first-order discrete Markov model is implemented as described in [9] with a state number of ten. The comparisons are made in terms of probability distribution, ACC, PACC and model parameter number.

The quantile-quantile plot of the simulated time series using the first-order discrete Markov model is shown in Fig. 11 (e). Although the trend of the quantile-quantile plot follows the straight line, it exhibits a staircase-like behavior due to the use of quantization in the discrete Markov model. By comparing Fig. 11 (d) and (e), it is apparent that in terms of the fit of probability distribution, the proposed LARIMA(0,1,1) model outperforms the ten-state first-order discrete Markov model.

The sample ACC and PACC of the measured time series and simulated ones using the LARIMA(0,1,1) and first-order discrete Markov model are shown in Fig. 12. The sample ACC of the LARIMA(0,1,1) model and Markov model match with that of the measurement. However, the PACC exposes the difference between the LARIMA model and Markov model. The sample PACC of the measured time series approaches zero for time lags larger than three. The sample PACC of the LARIMA model matches that of the measured time series for time lags up to three and approaches zero for time lags larger than three. However, the PACC of the Markov model approaches zero for time lags larger than one.

Recall that PACC describes the correlation between $Y(t)$ and $Y(t+k)$ when the mutual linear dependency of $Y(t+1)$, $Y(t+2)$, …, $Y(t+k-1)$ is removed. For a first-order discrete Markov model, the next state depends only on the current state, not the other states visited before. Therefore, the PACC of the discrete Markov model approaches zero for time lags larger than 1. However, due to its feedback loop (see Fig. 10 (b)), the LARIMA(0,1,1) model gives good accuracy of PACC at time lags larger than one. Therefore, the LARIMA(0,1,1) model gives better fit in PACC than the first-order discrete Markov model.

The fit of the first-order discrete Markov model to the measurement data can be improved by using higher order models, e.g. a second-order discrete Markov model. However, the number of parameters increases exponentially; the transition matrix of an n-state discrete Markov model of order

r has $n^r(n\text{-}1)$ parameters. This leads to 90 parameters for a first-order ten-state model ($n = 10$, and $r = 1$), and 900 parameters for a second-order ten-state model ($n = 10$, and $r = 2$). In contrast, the proposed LARIMA(0,1,1) model is described by only three parameters. Generally, the accuracy of a fitted model depends essentially on the amount of data available relative to the number of parameters to be estimated [15]. Thus, parsimonious models are preferred, and in some cases even required, when limited amount of data are available.

In summary, the proposed LARIMA(0,1,1) model is superior to the first-order transition matrix based discrete Markov model in terms of the probability distribution, the PACC, and the model parameter number.

In addition, the time-domain plot and power spectral density of the simulated time series using the proposed LARIMA(0,1,1) model are shown in Fig. 13 and Fig. 14, respectively. As mentioned in section III, the component corresponding to the diurnal period is not included in the present model. In the case of a strong diurnal period, the proposed model can be improved by applying a seasonal ARIMA model on the time series [12].

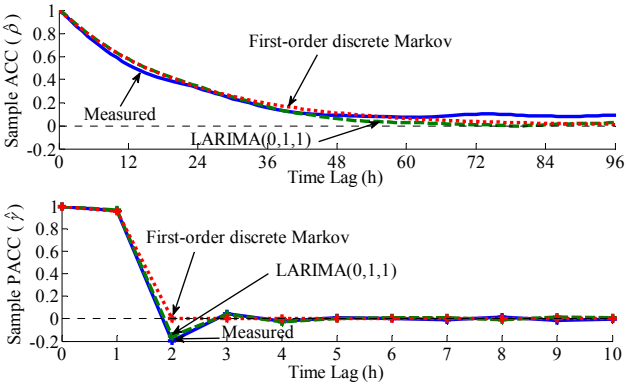

Fig. 12. Sample ACC (upper) and PACC (lower) of the measured time series, LARIMA(0,1,1) model, and first-order discrete Markov model.

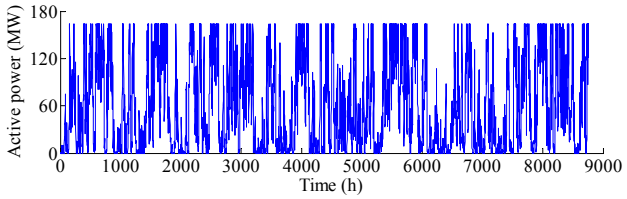

Fig. 13. Simulated wind power time series using the LARIMA(0,1,1) model.

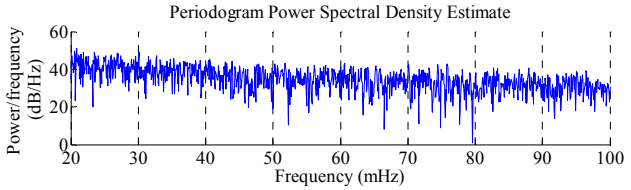

Fig. 14. Power spectral density of simulated wind power time series using the LARIMA (0,1,1) model.

D. Modeling of Seasonal Trend

So far a time series model that captures the averaged sample probability distribution, ACC, and PACC over a whole year has been developed. In order to take into account the seasonal trend, the same procedures can be applied to different parts of the time series representing different seasons or months. However, the length of each month (maximum 744 hours) of the time series is reduced approximately by a factor of 12 compared to that of a whole year (8760 hours). This shows the importance of a parsimonious model. A transition matrix based Markov model requires a large number of parameters. Thus, more data than a year are necessary to model the seasonal variability. In other words, the Markov model is not suitable when modeling seasonal trend with limited data. However, the proposed LARIMA(0,1,1) model relies on only three parameters, which is advantageous for modeling the seasonal trends.

Following the LARIMA(0,1,1) model in Fig. 10 (b), the estimated model parameters, θ_0, θ_1, and σ_a^2, for each month are shown in Fig. 15. It is noted that the values of the deterministic trend θ_0 are all negative in the summer months (May to October), and positive in the winter months (November to April). The phenomena reflect that the mean value of wind power generation is higher in winter months than in summer months. The monthly variation of θ_0 is large in the sense that its standard deviation is around 19 times of its mean. i.e. 0.0035. However, the monthly variation of θ_1 and σ_a^2 are quite small. The corresponding standard deviations are around 33% and 18% of the means, i.e. -0.225 and 1.165, respectively. This tends to indicate that the 12 monthly models can be connected by the same value of θ_1 and σ_a^2 but distinguished by θ_0. A longer time series measurement is required to further verify this conclusion. The monthly mean and variance of the simulated and measured time series are shown in Fig. 16. The results show that the model is able to capture the seasonal trend.

E. Further Discussions

The proposed LARIMA model captures the probability distribution, the ACC, the PACC and the seasonal trend adequately. However, as discussed in Section III, the 24 h period is ignored in the modeling of this wind power time series. The motivation for ignoring this effect is that the 24 h period is observed to be rather weak in the available data set shown in Fig. 5. Therefore, to adhere to the Principle of Parsimony, we leave out the explicit modeling of the diurnal period. In many cases, the diurnal period is also an important issue for modeling wind power generation. This is because of the strong diurnal period of electric loads that may be correlated (either positive or negative) with wind power generation. In the case of a time series that possesses a strong diurnal period or any other periods, the standard Box-Jenkins' seasonal ARIMA model can be applied [11], [12]. Accordingly, the seasonal LARIMA model can also be developed.

It is worth pointing out that the wind power data used for developing the LARIMA model are from a wind farm with fixed speed wind turbines. For wind farms with variable speed

wind turbines, both the probability distribution and the autocorrelation of the wind power may be different. The developed wind power model is only based on the data measured from the wind farm without the assumption of specific turbine types. Thus, the same modeling procedures can still be applied.

The proposed LARIMA model for wind power generation can be applied in the reliability assessment of power systems incorporating wind energy. The model can generate synthetic wind power time series, which are used in sequential Monte Carlo simulations to evaluate the adequacy of the system generation to meet future load demand. The proposed wind power model has a good fit in probability density function, especially on the tail regions. This fact, as well as the model's computational simplicity, makes the model especially suitable and reliable for Monte Carlo simulations.

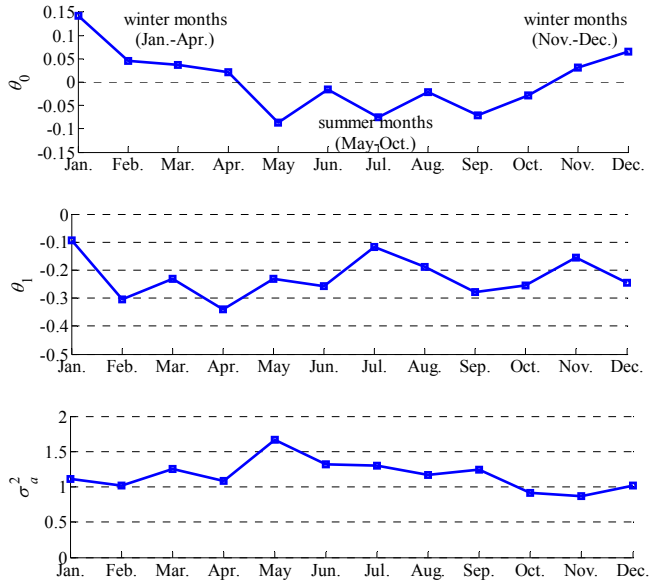

Fig. 15. ARIMA(0,1,1) based model parameters for each month: θ_0 (upper), θ_1 (middle), and σ_a^2 (lower).

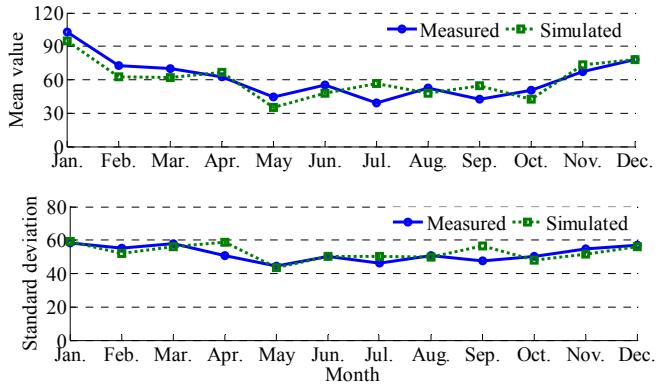

Fig. 16. Monthly mean (upper) and standard deviation (lower) of one-year measured (solid-circle) and simulated (dotted-square) time series considering seasonal trend in the model.

VI. Conclusions and Future Work

This paper contributes to the statistical analysis and modeling of a nonstationary and bounded wind power time series. The analyses indicate that the examined wind power time series is a nonstationary random process with high fluctuation and temporal correlation. However, the time series has a rather weak 24 h period. It is found that its probability distribution does not resemble a standard distribution such as an exponential, or a Gaussian distribution.

A novel LARIMA model is proposed for the wind power time series. The LARIMA model is obtained by introducing a limiter into a standard ARIMA model to represent the upper and lower bounds of the wind power generation. The proposed model characterizes the wind power generation by three unknown parameters, representing the mean level (θ_0), temporal correlation (θ_1), and driving noise (σ_a^2) of the wind power generation, respectively. The proposed LARIMA(0,1,1) model outperforms the ARMA(1,1) model with limiter and the LARMA(1,1) model when evaluating the probability distribution. The proposed LARIMA(0,1,1) model also outperforms the first-order transition matrix based discrete Markov model when evaluating the probability distribution, PACC and model parameter number. The monthly variation of the wind power time series is modeled by applying the LARIMA(0,1,1) model to the individual months of the time series. It is found that the monthly variation is mainly caused by different mean level (θ_0) of wind power in each month. The monthly variation in θ_1 and σ_a^2 is observed to be relatively small.

The developed stochastic wind power model can facilitate the understanding and analysis of the impact of stochastic wind power generation on power system planning and reliability studies. The sensitivity analysis of the stochastic wind power generation with respect to the variation in mean level, temporal correlation and driving noise can be readily carried out using the proposed model. Future work on the proposed LARIMA model includes the derivation of analytical expressions for the probability density function as well as its moments. If wind power measurements of longer periods are available, the year-to-year variation can be modeled and used to improve the accuracy of the model for long-term planning applications.

Acknowledgment

The authors would like to thank the Danish distribution company SEAS-NVE for kindly providing the measurement data from the Nysted offshore wind farm.

References

[1] H. L. Willis and W. G. Scott, *Distributed Power Generation: Planning and Evaluation*. Boca Raton: CRC Press, 2000.

[2] R. Billinton and W. Wangdee, "Reliability-based transmission reinforcement planning associated with large-scale wind farms," *IEEE Trans. Power Systems*, vol. 22, pp. 34-41, Feb. 2007.

[3] R. Billinton, H. Chen and R. Ghajar, "Time-series models for reliability evaluation of power systems including wind energy," *Microelectron. Reliab.*, vol. 36, pp. 1253-1261, 1996.

[4] B. G. Brown, R. W. Katz, and A. H. Murphy, "Time series models to simulate and forecast wind speed and wind power," *J. Climate and Applied Meteorology*, vol. 23, pp. 1184-1195, May 1984.
[5] A. Shamshad, M. A. Bawadi, W. M. A. Wan Hussin, T. A. Majid, and S. A. M. Sanusi, "First and Second order Markov chain models for synthetic generation of wind speed time series," *Energy*, vol. 30, pp. 693-7081, 2005.
[6] F. Castro Sayas and R. N. Allan, "Generation Availability Assessment of Wind Farms," *IEE Proc. Generation, Transmission, Distribution*, vol. 143, pp. 507-518, Sep. 1996.
[7] N. B. Negra, O. Holmstrøm, B. Bak-Jensen and P. Sørensen, "Model of a synthetic wind Speed time series generator," *Wind Energy*, vol. 11, pp. 193-209, 2008.
[8] T. Kitagawa and T. Nomura, "A wavelet-based method to generate artificial wind fluctuation data," *Journal of Wind Engineering and Industrial Aerodynamics*, vol. 91, pp. 943-964, 2003.
[9] G. Papaefthymiou and B. Klöckl, "MCMC for wind power simulation," *IEEE Trans. Energy Conversion*, vol. 23, pp. 234-240, Mar. 2008.
[10] A. Stuart and J. K. Ord, *Kendall's Advanced Theory of Statistics: Volume 1 Distribution Theory*. 6th ed. London: Edward Arnold, 1993.
[11] G. E. P. Box, G. M. Jenkins and G. C. Reinsel, *Time Series Analysis: Forecasting and Control*. 3rd ed. New Jersey: Prentice-Hall, 1994.
[12] W. W. S. Wei, *Time Series Analysis: Univariate and Multivariate Methods*. Redwood City: Addison-Wesley, 1990.
[13] A. Papoulis and S. U. Pillai, Probability, Random Variables and Stochastic Processes. 4th ed. New York: McGraw-Hill, 2002.
[14] A. Leon-Garcia, Probability, Statistics, and Random Process for Electrical Engineering. 3rd ed. New Jersey: Pearson Prentice Hall, 2009.
[15] H. Linhart and W. Zucchini, Model Selection. New York: John Wiley & Sons, 1986.

VII. BIOGRAPHIES

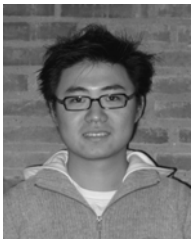

Peiyuan Chen (S'2007) received his B.Eng. degree in Electrical Engineering from Zhejiang University, China, in 2004 and M.Sc. degree in Electric Power Engineering from Chalmers University of Technology, Sweden, in 2006. From August of 2005 to June of 2006, he was also with ABB Corporate Research, Sweden. He is currently pursuing his Ph.D. degree at Aalborg University, Denmark. He is working on the probabilistic modeling of power systems with integration of renewable energy based distributed generation. His focus is on stochastic models of wind power generation and their applications in power system operation and planning.

Troels Pedersen (S'2004) received the M.Sc.E. degree in digital communications and the Ph.D. degree in wireless communications from Aalborg University, Denmark, in 2004 and 2009, respectively. He is currently an assistant professor at the Department of Electronic Systems, Aalborg University. His research interests lie in the area of statistical signal processing and communication theory, including sensor array signal processing, wireless localization techniques, radio channel modelling, and radio channel sounding.

Birgitte Bak-Jensen (M'1988) received her M.Sc. degree in Electrical Engineering in 1986 and a Ph.D. degree in "Modelling of High Voltage Components" in 1992, both degrees from Institute of Energy Technology, Aalborg University, Denmark. From 1986-1988 she was with Electrolux Elmotor A/S, Aalborg, Denmark as an Electrical Design Engineer. She is an Associate Professor in the Institute of Energy Technology, Aalborg University, where she has worked since August 1988. Her fields of interest are modelling and diagnosis of electrical components, power quality and stability in power systems. During the last years, integration of dispersed generation to the network grid has become one of her main fields, where she has participated in many projects concerning wind turbines and their connection to the grid.

Zhe Chen (M'1995, SM'1998) received the B.Eng. and M.Sc. degrees from Northeast China Institute of Electric Power Engineering, Jilin City, China, and the Ph.D. degree from University of Durham, U.K. He was a Lecturer and then a Senior Lecturer with De Montfort University, U.K. Since 2002, Dr. Chen became a Research Professor and is now a Professor with the Department of Energy Technology, Aalborg University, Denmark. He is the coordinator of Wind Power System Research program at the Institute of Energy Technology, Aalborg University. His background areas are power systems, power electronics and electric machines; and his main current research areas are wind energy and modern power systems. Dr Chen has more than 190 publications in his technical field. He is an Associate Editor (Renewable Energy) of the IEEE Transactions on Power Electronics. Dr. Z. Chen is a Member of the Institution of Engineering and Technology (London, U.K.), and a Chartered Engineer in the U.K.